Numerical Prediction of Valve Coefficients and Unsteady Cavitating Turbulent Flow in a Ball Valve

Yogesh Gawas, Dr. Vilas R. Kalamkar, Vijay Mali

***Abstract*—**Ball valve, a rotational motion valve uses ball shaped disk. It is used for on/off or throttling operations. It offers the minimum resistance to flow. To investigate the valve performance and its characteristics, the flow through the valve is studied using numerical technique. In this paper the numerical simulations were performed using commercial code FLUENT, to study the flow patterns and to estimate the valve sizing coefficient, torque coefficient and cavitation index for investigation of cavitating flows. These simulations were performed at different pressure drops and for varying percentage opening of the valve.

***Keywords*—**Ball Valve, Cavitation, Numerical Simulation, Valve Coefficients.

I. Introduction

BALL valve is a quarter-turn valve that features a spherical closure device. As the ball move radially across the seal, the opening in the ball is exposed, which allow the flow. Ball valve is also categorized as high-pressure recovery valve. At intermediate openings, there are two throttling ports in series, one at the inlet and other at the outlet of the ball. Hence the system experiences double pressure drop, due to which ball valve has better cavitation characteristics.

Computational Fluid Dynamic (CFD) technique, are much developed and are used as an important tool in scientific research and also in industrial engineering designs. By now, the CFD simulation by commercial software had proved their ability to predict the flow characteristics. The flow pattern inside the valve, formation of vortices, and complex phenomenon like cavitation can be visualized by CFD techniques.

CFD has become a popular tool for design of fluid machinery, valves, heat exchanger and many other devices. There have been many reports on valves, in which different flow phenomena were analyzed using CFD technique. The commercial code, STAR-CD™, was used to investigate fluid flows through a ball valve and to estimate the important coefficients [1]. Using FLUENT™, investigation of flow around a V-sector ball valve was performed [2]. A three dimensional numerical analysis, was performed to reveal the velocity field, pressure distributions in a butterfly valve by using FLUENT™ [3]. Using AVL-Fire™, the flow containing the bubbles in a ball valve was analyzed [4]. To perform three dimensional analysis, to estimate pressure drop, flow coefficient and hydrodynamic torque coefficient in a butterfly valve ANSYS CFX™ was used [5]. Implementing mixture model of FLUENT™, the cavitating turbulent flow for two dimensional NACA0009 hydrofoil was analyzed [6].

In this research the main objective is to model the fluid domain of 10 inch ball valve, along with the prescribed length of upstream and downstream piping system. Commercial package ICEM-CFD 12.0 was used as pre-processing tool, while FLUENT 12.0 was used as solver and for post-processing. FLUENT provides a three dimensional numerical simulation of water through the ball valve and the fluid domain, and also helps to estimate the pressure drop, volume flow rate, sizing coefficient , torque coefficient, and cavitation index.

Fig. 1 Trunnion type full port ball valve

Yogesh Gawas is a post -graduation student with Sardar Patel College of Engineering, University of Mumbai, Mumbai, India. Phone: +91 9969468424, e- mail: g15engineering@yahoo.co.in, g15engineering@gmail.com

Dr Vilas R. Kalamkar is a Professor with Department of Mechanical Engineering at Sardar Patel College of Engineering, University of Mumbai, Mumbai, India. Phone: +91 9819591384, e-mail: vilas.kalamkar@gmail.com

Vijay Mali is Director with Centre for Computational Technologies (CCTech) Pvt. Ltd., Pune. India. Phone: +91 9850861178, e-mail: vijay@cctech.co.in

TABLE I
NOMENCLATURE

Symbol	Quantity	Units
Ct	Torque Coefficient	
Cv	Valve sizing Coefficient	m^3/hr
CI, CI₁	Cavitation Index	
D	Nominal Diameter of Ball Valve	mm
$\vec{F}_B$	Body Force	N
f	Mass Fraction	
k	Turbulence Kinetic Energy	m^2/s^2
n	Number of Phase	
P_{sat}	Saturation Pressure	Pa
P_{turb}	Turbulence-Induced Pressure	Pa
Q	Volume Flow Rate	m^3/s
S.G	Specific Gravity	
T	Hydrodynamic Torque	N-m
u	Mean Velocity	m/s
$\vec{v}$	Mass Averaged Velocity	m/s
α	Volume Fraction	
γ	Effective exchange coefficient	
μ	Viscosity	Kg/m-s
ρ	Density	Kg/m^3
σ	Surface Tension Coefficient	N/m
ΔP	Pressure Drop	Pa
$-\rho\overline{u_i' u_j'}$	Reynolds Stress	$Kg/m.s^2$

II. VALVE SIZING COEFFICIENT, INHERENT CHARACTERISTICS, TORQUE COEFFICIENT, AND CAVITATION INDEX

A. Valve Sizing Coefficient (Cv)

It is defined as quantity of water in US gallons at 60°F that will pass through the valve each minute with a 1 psi pressure drop across it. It is also a measure of capacity of valve, which takes account of its size and natural restriction to flow through the valve. Also it is a dimensional value. It can be calculated by following equation.

$$Cv = 1.16 \times Q \times \sqrt{\frac{S.G}{\Delta P}} \quad (1)$$

B. Inherent Characteristic

It is a relationship between sizing coefficient and closure member (disk) travel at constant pressure drop. Conducting flow characteristics test at a constant pressure drop provides a systematic way of comparing one valve characteristics to another. Typical valve characteristics conducted in this manner are named as linear, quick opening, and equal percentage characteristics.

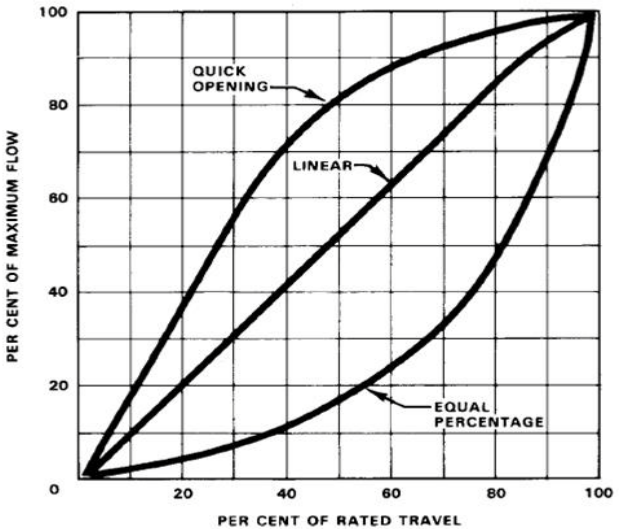

Fig. 2 Inherent valve characteristics

Linear Characteristic: For equal increments of travel there are equal increments of flow coefficient and is represent by a straight line.

Quick Opening Characteristic: A maximum flow coefficient is achieved with minimal closure member travel.

Equal Percentage Characteristic: For equal increments of travel there will be ideally equal percentage change of flow coefficient.

C. Torque Coefficient (Ct)

Forces required to open/close a quarter-turn valves are caused by friction and hydrodynamic forces. Friction forces act at the valve seat and bearing surfaces. Hydrodynamic torque is caused by forces induced by the flowing fluid. Torque coefficients are dimensionless entities, varies with valve opening position. It is calculated by the following equation.

$$Ct = \frac{T}{D^3 \times \Delta P} \quad (2)$$

D. Cavitation Index (CI)

Cavitation Index is a parameter derived from the dimensional analysis, which corresponds to the intensity of cavitation. It is defined as the ratio of forces trying to suppress cavitation to the force trying to cause it. For valves and other devices that create a pressure drop, Cavitation Index can be further defined in several ways as explained further.

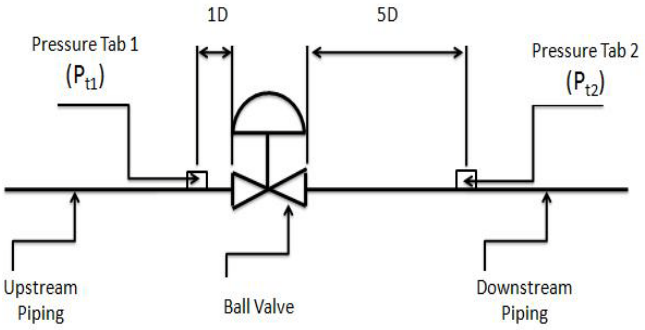

Fig. 3 Schematic diagram of ball valve and piping system

Pressure Tab 1 is installed one diameter upstream from valve. Pressure Tab 2 is installed five diameters downstream from valve, fig. 3. If the reference pressure in numerator is upstream pressure, P_{t1} then

$$CI = \frac{P_{t1} - P_{sat}}{\Delta P} \tag{3}$$

If the reference pressure in numerator is downstream pressure, P_{t2} then

$$CI_1 = \frac{P_{t2} - P_{sat}}{\Delta P} \tag{4}$$

Equation (4) is a much preferred form over (3), since downstream pressure is the pressure closer to zone, where cavitation actually occurs. Therefore downstream pressure, more directly influences the cavitation process. Equation (3) & (4) are related by the following equation.

$$CI = CI_1 + 1 \tag{5}$$

Table II shows the typical range of Cavitation Index [7].

TABLE II
CAVITATION INDEX GENERAL RANGE

Cavitation Index Range	Intensity Of Cavitation
CI≥ 2	No Cavitation
1.7 < CI < 2	No Cavitation
1.5 < CI < 1.7	Some Cavitaiton
1 < CI < 1.5	Sever Cavitation
CI ≤ 1 or negative	Flashing

III. CFD MODELLING

A. Model Description

For this study a10 inch nominal diameter ball valve geometric model was initially provided in IGES format and then it was imported using ICEM-CFD 12.0

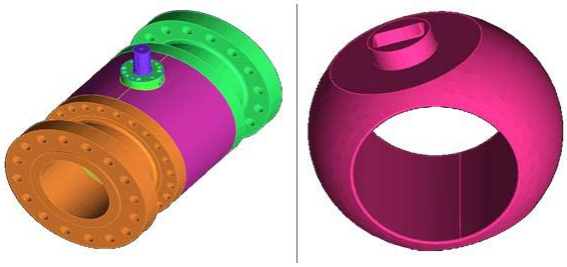

Fig. 4 Ball valve and the disk (ball)

The required fluid domain was then extracted from the geometry and the prescribed length of piping system was added on upstream and downstream side.

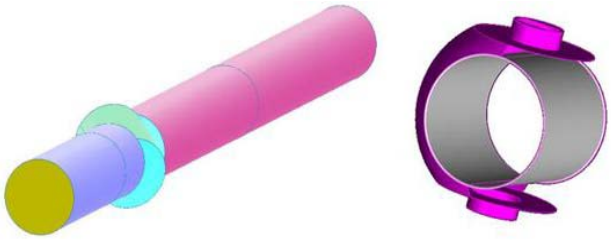

Fig. 5 Extracted fluid domain and upstream and downstream piping system

To perform simulations at different percentage opening, different geometries were created as per angular rotation of ball valve. Accuracy of simulation mainly depends on quality of grid, hence to get better results, tetrahedral mesh generated using ICEM-CFD 12.0, were converted to polyhedral mesh using FLUENT 12.0

B. Numerical Approach

Basic Flow Model: Working fluid is water, hence incompressible and viscous fluid flows through the ball valve. Pressure drop between inlet and outlet being very high induces high velocity flow, hence flow studied is turbulent in nature.

Turbulence Model: To capture turbulence, Reynolds Averaged Navier-Stokes (RANS) equation is utilized. Its common form is written as;

$$\frac{\partial \rho}{\partial t} + \frac{\partial}{\partial x_i}(\rho u_i) = 0 \tag{6}$$

$$\frac{\partial}{\partial t}(\rho u_i) + \frac{\partial}{\partial x_i}(u_i u_j) = -\frac{\partial p}{\partial x_i} + \frac{\partial}{\partial x_j}\left[\mu\left(\frac{\partial u_i}{\partial x_j} + \frac{\partial u_j}{\partial x_i} - \frac{2}{3}\delta_{ij}\frac{\partial u_l}{\partial x_l}\right)\right] + \frac{\partial}{\partial x_i}\left(-\rho\overline{u'_i u'_j}\right) \tag{7}$$

Where u is the mean velocity and the subscript, i, j=1~3, refers to Reynolds-averaged components in three directions respectively. These Reynolds Stresses, $-\rho\overline{u'_i u'_j}$, must be modeled in order to close the equation.

Reynolds Averaged Navier-Stokes equations modify the original unsteady Navier-Stokes equations by introducing averaged and fluctuating terms, which acts like additional stresses in the fluid. These terms, called Reynolds stresses, are difficult to determine directly and so become further unknowns. The Reynolds stresses need to be modeled by additional equations of known quantities in order to achieve "closure". For this study realizable k-ε turbulence model is utilized. This model satisfies certain mathematical constraints on the Reynolds Stresses which are consistent with the physics of turbulent flow. This model is more accurate and robust. Standard wall function approach is utilized for the near wall treatment. Standard wall function, provide reasonably accurate predictions for majority high Reynolds Number wall bounded flows.

Cavitation Modeling:

1. Introduction to Cavitation and Flashing: When the internal pressure of liquid at some points falls below the vapor pressure and vapor bubbles are formed and at some point downstream, pressure rise above the vapor pressure again. As this pressure recovers, so the bubbles collapse and cavitation takes place.

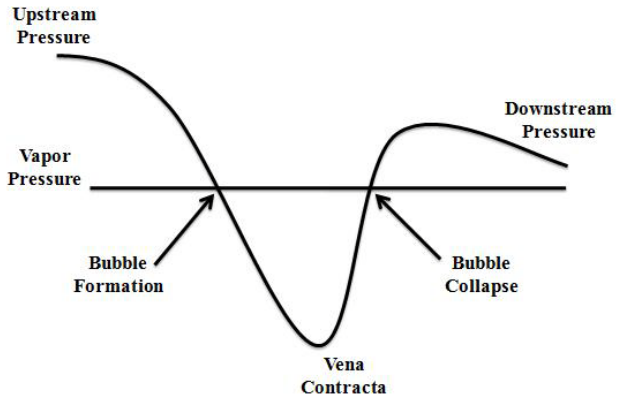

Fig. 6 Pressure variation for cavitation process

Flashing is a condition that occurs where pressure falls below vapor pressure and remains below it. There are then two phases flowing (liquid and its vapor) downstream. It is more severe as compared to cavitation.

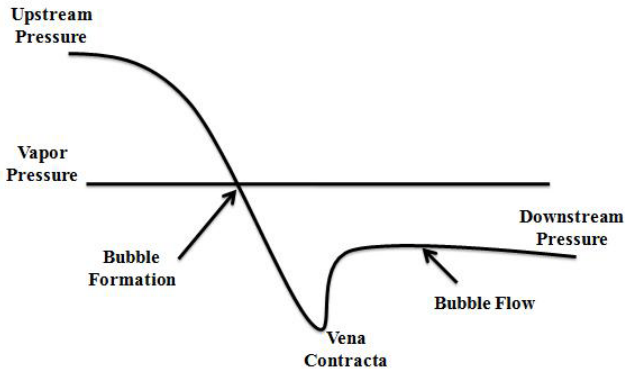

Fig. 7 Pressure variation for flashing process

Cavitation and flashing process occurs at constant temperature and reducing pressure. Because of these processes a very large and steep density variation occurs in low pressure region.

2. Role of Non-Condensable Gases/Nuclei: The term nuclei is other name for gas bubbles or voids in the liquid. For cavitation to occur, there must be nuclei present. If liquid was completely deaerated (i.e. no nuclei), then liquid will sustain tension and would not cavitate when pressure dropped to vapor pressure. Liquid will cavitate far below the normal liquid vapor pressure

3. Cavitation Model in FLUENT: FLUENT's current cavitation model is available only with Mixture Model [8]. This model is based on Full Cavitation Model. It accounts for all first order effects (i.e. phase change, bubble dynamics, turbulent pressure fluctuations and non-condensable gases). Further this model is divided as, Basic Cavitation Model, and Extended Cavitation Model. For this study Basic Cavitation Model is used, it includes fundamental modeling approach and standard two phase cavitation model. It provides mass transport between a single liquid and its vapor only. Full cavitation model utilizes modified Rayleigh-Plesset equations for bubble dynamics and includes effects of turbulent pressure fluctuations and non-condensable gases.

4. Governing Equations Used for Cavitation Model:

i. Continuity Equation for Mixture Model:

$$\frac{\partial}{\partial t}(\rho_m) + \nabla.(\rho_m \overrightarrow{v_m}) = 0 \tag{8}$$

Where $\overrightarrow{v_m}$ = mass averaged velocity

$$\overrightarrow{v_m} = \sum_{k=1}^{n} \frac{\alpha_k \rho_k \overrightarrow{v_k}}{\rho_m}$$

ρ_m = mixture density

$$\rho_m = \sum_{k=1}^{n} \alpha_k \rho_k$$

α_k, ρ_k and $\overrightarrow{v_k}$ = volume fraction, density and mass averaged velocity

ii. Momentum Equation for Mixture Model:

$$\frac{\partial}{\partial t}(\rho_m \vec{v}_m) + \nabla.(\rho_m \vec{v}_m \vec{v}_m) = -\nabla p + \nabla.\left[\mu_m\left(\nabla \vec{v}_m + \nabla \vec{v}_m^{\,T}\right)\right] + \rho m \vec{g} + \vec{F} + \nabla\left(\sum_{k=1}^{n} \alpha_k \rho_k \overrightarrow{v_{dr,k}} \overrightarrow{v_{dr,k}}\right) \tag{9}$$

Where μ_m = Mixture viscosity

$$\mu_m = \sum_{k=1}^{n} \alpha_k \mu_k$$

$$\overrightarrow{v_{dr,k}} = \overrightarrow{v_k} - \overrightarrow{v_m}$$

iii. Vapor Transport Equation: Working fluid is assumed to be a mixture of liquid, its vapor and non-condensable gases. Standard governing equations in Mixture Model and Mixture Turbulence Model describe the flow and account for the effects of turbulence. Vapor transport equation governs the vapor mass fraction 'f', given by

$$\frac{\partial}{\partial t}(\rho_m f) + \nabla(\rho_m \vec{v}_v f) = \nabla(\gamma \nabla f) + R_e - R_c \quad (12)$$

Where ρ_m = Mixture density,
$\vec{v}_v$ =velocity vector of vapor phase,
γ =effective exchange coefficient,
R_e & R_c = vapor generation and condensation rate terms, derived from Rayleigh-Plesset equations and limiting bubble size consideration. These rates are functions of instantaneous local static pressure and turbulence-induced pressure. since turbulence has significant effect on cavitating flows, the phase change threshold pressures is raised from saturation pressure to a new function which is summation of saturation pressure and turbulence-induced pressure. Equations are as follows

When $p < p_v$

$$R_e = C_e \frac{\sqrt{k}}{\sigma} \rho_l \rho_v \sqrt{\frac{2(p_v - p)}{3\rho_l}} (1 - f_v - f_g) \quad (13)$$

When $p > p_v$

$$R_c = C_c \frac{\sqrt{k}}{\sigma} \rho_l \rho_l \sqrt{\frac{2(p - p_v)}{3\rho_l}} f_v \quad (14)$$

$$p_v = \frac{1}{2}(p_{sat} + p_{turb})$$

$$p_{turb} = 0.39\rho k$$

$$\rho_m = \alpha_v \rho_v + \alpha_g \rho_g + (1 - \alpha_v - \alpha_g)\rho_l$$

Where Ce = 0.02, Cc = 0.01,
k = local turbulence kinetic energy,
σ = surface tension coefficient of the liquid,
f_v & f_g = mass fraction of vapor and non-condensable gases,
p_{sat} = saturation pressure,
p_{turb} = turbulence-induced pressure,
ρ_v, ρ_g & ρ_l = density of vapor, non-condensable gases and liquid.
α_v & α_g = volume fraction of vapor and non-condensable gases.

C. Working Fluid, Operating Condition, and Boundary Condition: Table III shows the working fluid used in analysis, the operating pressure, type of boundary conditions used, phases involved, and vaporization pressure.

TABLE III
BOUNDARY CONDITIONS

	For Numerical Prediction of	
	Valve sizing and Torque Coefficient	Cavitating Flow
Working Fluid	Water	Water, Water Vapor, Non-Condensable Gases
Operating Condition	101325 Pa	101325 Pa
Phases	Single Phase Flow	Two Phase Flow (Water, Water Vapour)
Vaporization Pressure		3564 Pa at 300K
Inlet Boundary Condition	Pressure Inlet Boundary Condition	Pressure Inlet Boundary Condition
Outlet Boundary Condition	Pressure Outlet Boundary Condition	Pressure Outlet Boundary Condition

IV. RESULTS AND DISCUSSION

A. Results of velocity field of a single phase fluid flow, Valve Sizing Coefficient, Hydrodynamic Torque and Torque Coefficient: Following figures shows the contours of velocity on x-z plane for a pressure drops of 20.7 bar (300 psi) and different percentage opening of ball valve (10%, 20%, 30%, 40%, 50%, 60%, 70%, 80%, 90%).

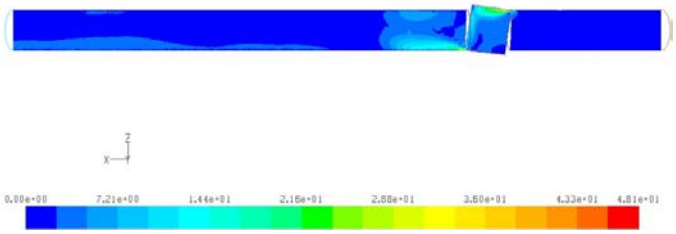

Fig. 8 Velocity contour plot for 10 percent opening

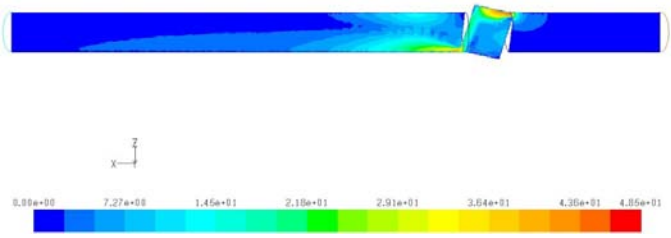

Fig. 9 Velocity contour plot for 20 percent opening

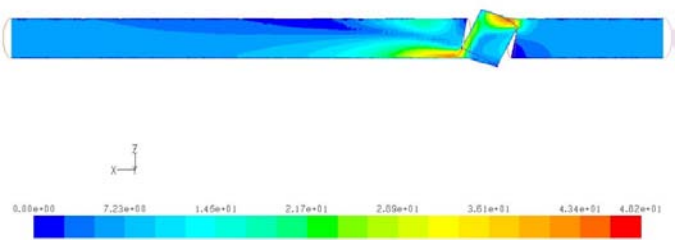

Fig. 10 Velocity contour plot for 30 percent opening

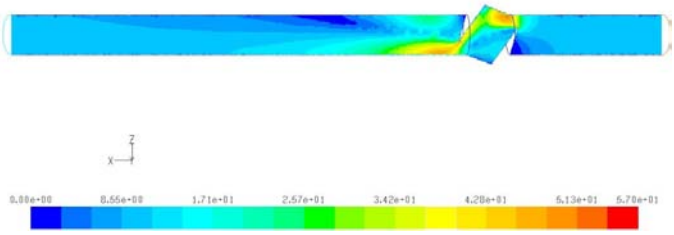

Fig. 11 Velocity contour plot for 40 percent opening

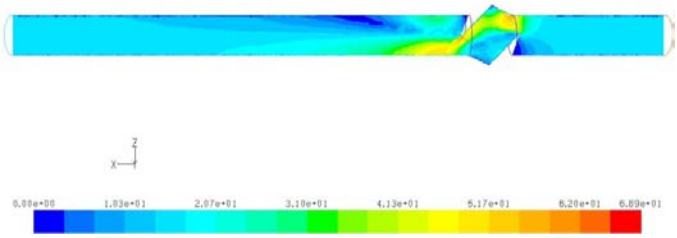

Fig. 12 Velocity contour plot for 50 percent opening

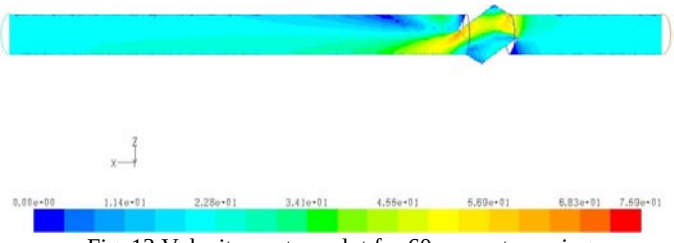

Fig. 13 Velocity contour plot for 60 percent opening

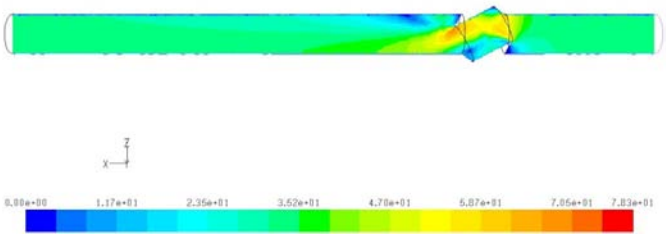

Fig. 14 Velocity contour plot for 70 percent opening

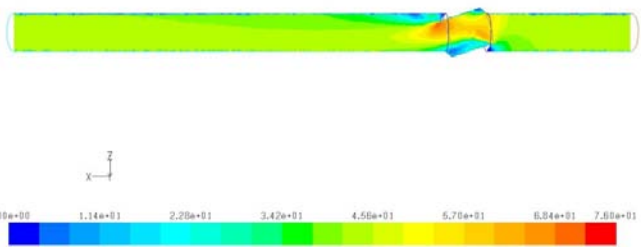

Fig. 15 Velocity contour plot for 80 percent opening

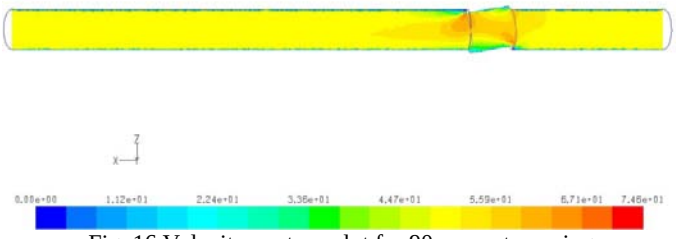

Fig. 16 Velocity contour plot for 90 percent opening

Similar other simulations were performed at 19.3 bar (280 psi), 16.55 bar (240 psi), 11.7 bar (170 psi), 7.6 bar (110 psi) and different percentage opening of valve.

Fig. 17 shows Valve Sizing Coefficient graph. The experimental value of Valve Sizing Coefficient for 100 percent opening is 3180 [8]. The value obtained from simulation result for 100 percent opening is 3086. Hence experimental Cv values and Numerically obtained values can be compared for validation. Curve characteristic signifies that Cv values depends only on geometry and are independent of flow conditions. Cv reduces as valve is closed.

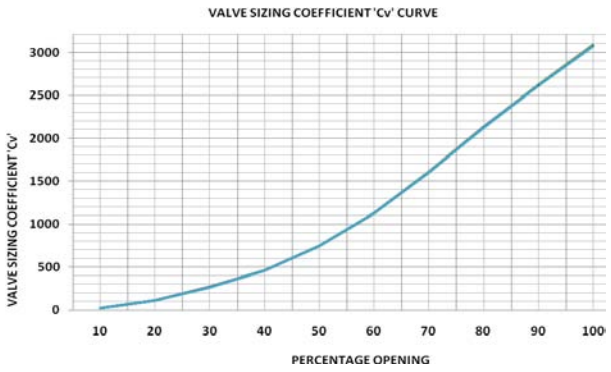

Fig. 17 Graph of variation of valve sizing coefficient

Fig. 18 shows a graph between percent of valve sizing coefficient and percentage valve opening. From this graph it is observed that the valve under study has 'Equal Percentage' inherent characteristic.

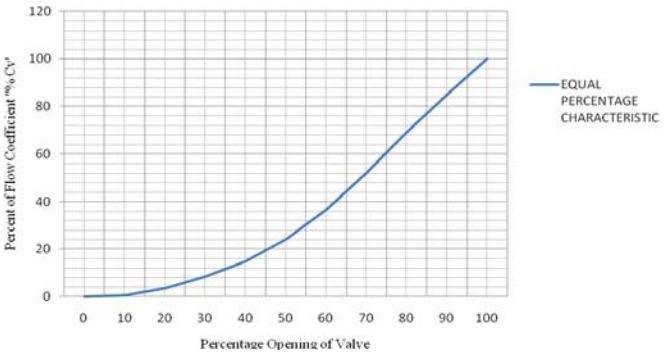

Fig. 18 Graph of equal percentage characteristics

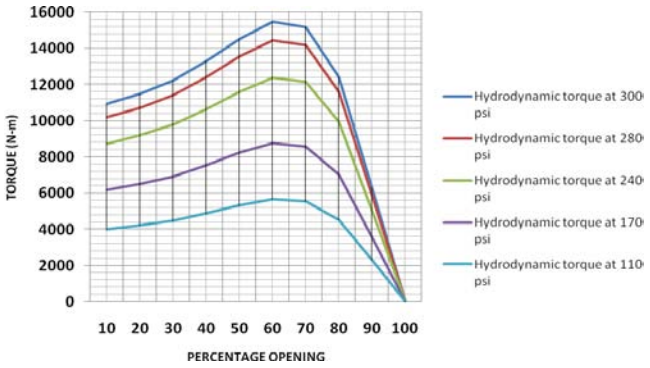

Fig. 19 Graph of variation of hydrodynamic torque

Hydrodynamic torque reduces with pressure drop. As valve is closed (i.e. reduction in percentage opening) hydrodynamic torque increases to a maximum value and then reduces. Though the hydrodynamic torque changes with pressure drop and valve opening, but in all cases, it is seen that peak point for hydrodynamic torque (maximum torque) is at 60% percent opening of valve.

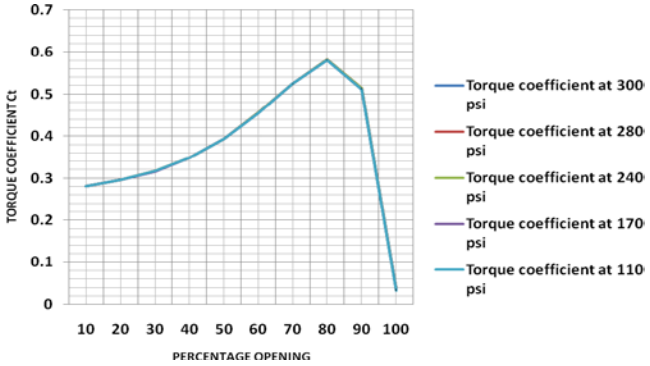

Fig. 20 Graph of variation of torque coefficient

Torque coefficient remains constant even as pressure varies. As valve is closed torque coefficient increases to a maximum value and then reduces. Maximum torque coefficient occurs at 80% opening for this valve.

B. Results pressure variation, velocity field, volume fraction of vapour and cavitation index for two phase cavitating turbulent flow:

Following figures shows the graph of absolute pressure variation along the pipe length, contour plots of volume fraction for vapor and velocity of mixture. These results are plotted for pressure drop of 20.7 bar (300 psi), 7.6 bar (110 psi), and different percentage opening of ball valve (10%, 20%, 30%, 40%, 50%, 60%). Similar other simulations were performed at 19.3 bar (280 psi), 16.55 bar (240 psi), 11.7 bar (170 psi), and different percentage opening of valve.

1. Results for 20.7 bar (300 psi) pressure drop:

a) *Graphs of pressure variation:* The pressure shown in graphs is static pressure in absolute terms. These graphs show the variation in static pressure caused due to variation in velocity. Double pressure drop in ball valve, one at the valve inlet and other at the valve outlet is also visible. These curves represent the occurrence of cavitation, as the local static pressure falls below vaporization pressure.

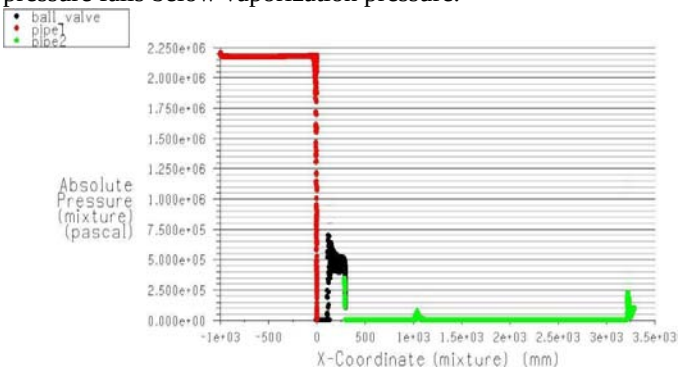

Fig. 21 Graph of absolute pressure variation for 10 percent opening

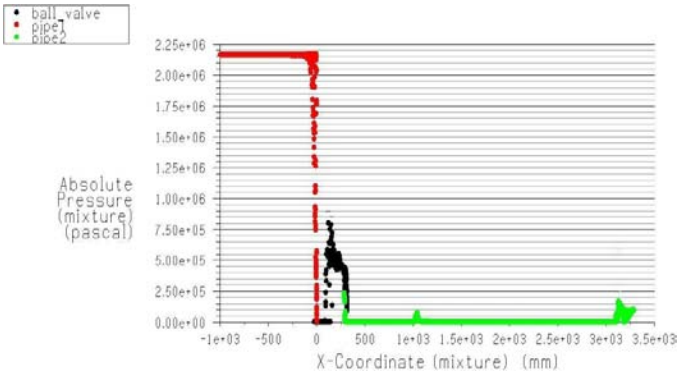

Fig. 22 Graph of absolute pressure variation for 20 percent opening

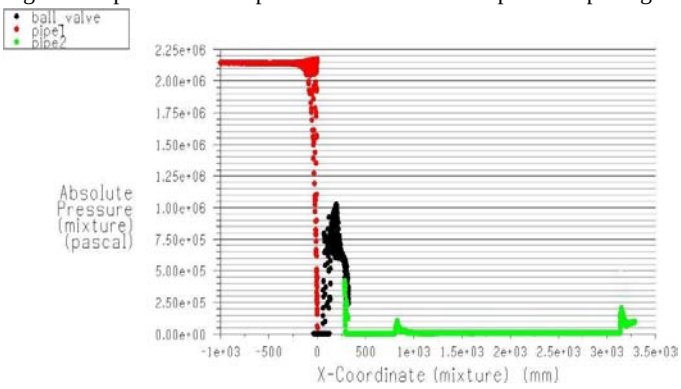

Fig. 23 Graph of absolute pressure variation for 30 percent opening

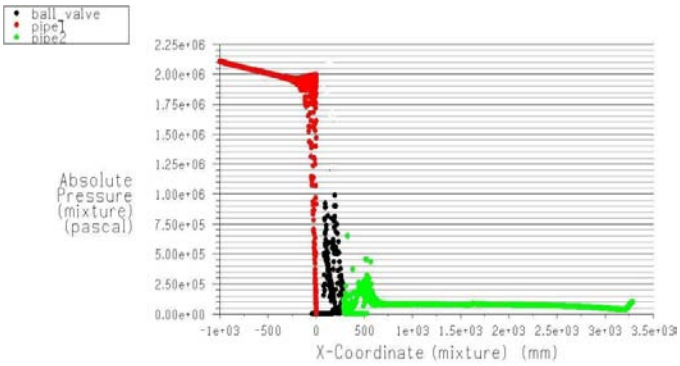

Fig. 24 Graph of absolute pressure variation for 40 percent opening

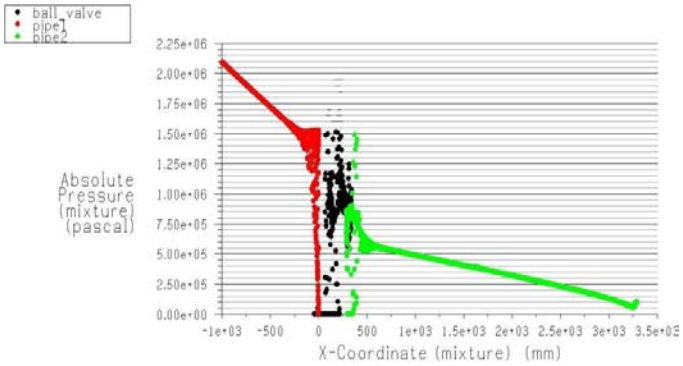

Fig. 25 Graph of absolute pressure variation for 50 percent opening

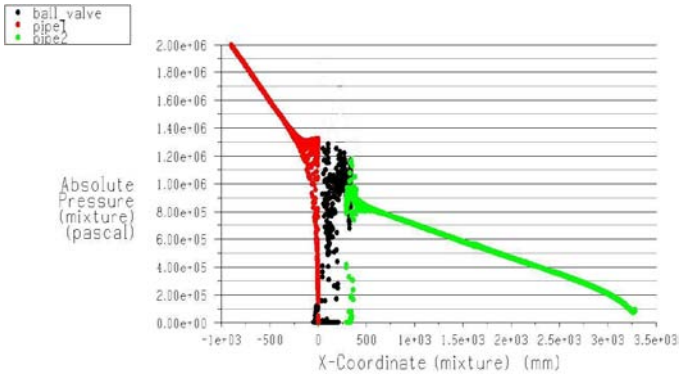

Fig. 26 Graph of absolute pressure variation for 60 percent opening

b) Velocity Contours on x-z plane: High velocity flows causes reduction in static pressure, if pressure falls below vapor pressure than cavitation occurs.

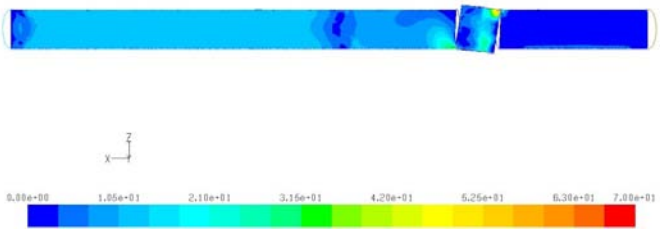

Fig. 27 Mixture velocity contour plot for 10 percent opening

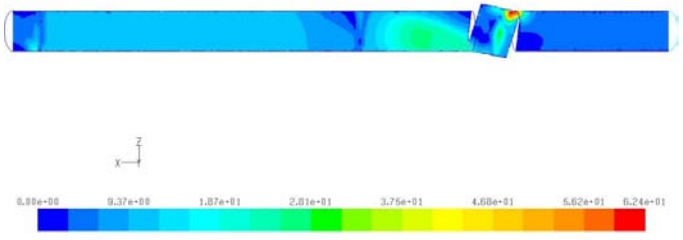

Fig. 28 Mixture velocity contour plot for 20 percent opening

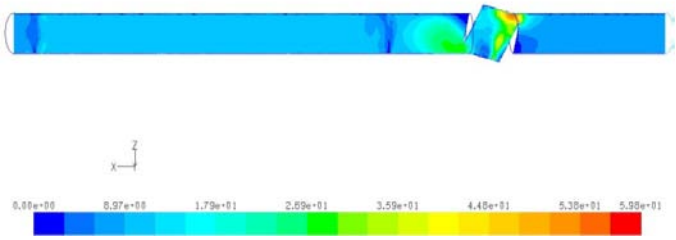

Fig. 29 Mixture velocity contour plot for 30 percent opening

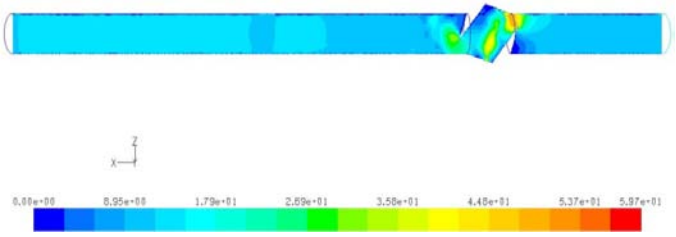

Fig. 30 Mixture velocity contour plot for 40 percent opening

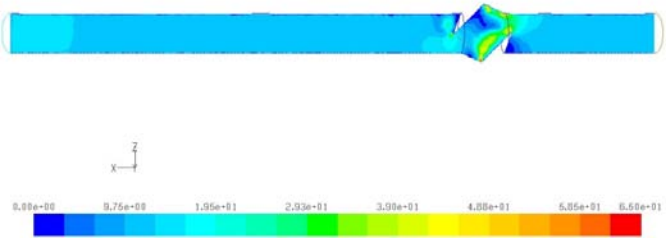

Fig. 31 Mixture velocity contour plot for 50 percent opening

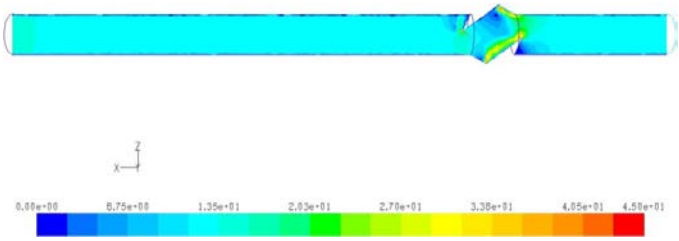

Fig. 32 Mixture velocity contour plot for 60 percent opening

c) *Contour of Volume Fraction for Vapor Phase:* These contours represent the actual Cavitation or Flashing zones in the ball valve and the piping system. Also downstream piping system is severely affected by cavitating flow. Volume fraction for vapor phase varies between 0 and 1. 0 represents no vapor formation or no cavitation, whereas, 1 represents vapor flow (i.e. cavitating flow).

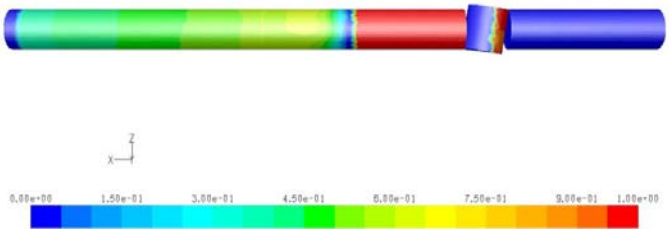

Fig. 33 Volume fraction of vapor phase for 10 percent opening

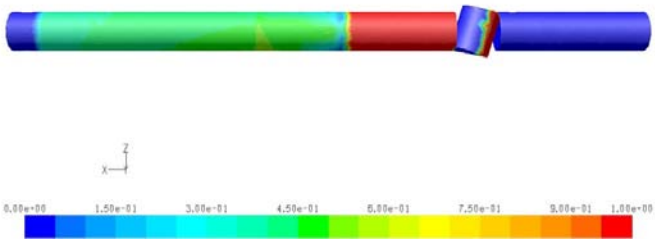

Fig. 34 Volume fraction of vapor phase for 20 percent opening

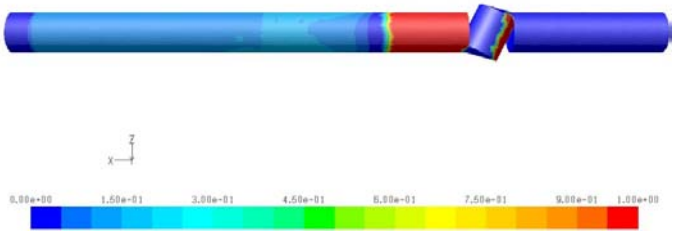

Fig. 35 Volume fraction of vapor phase for 30 percent opening

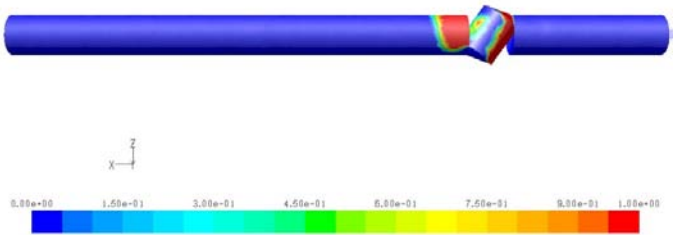

Fig. 36 Volume fraction of vapor phase for 40 percent opening

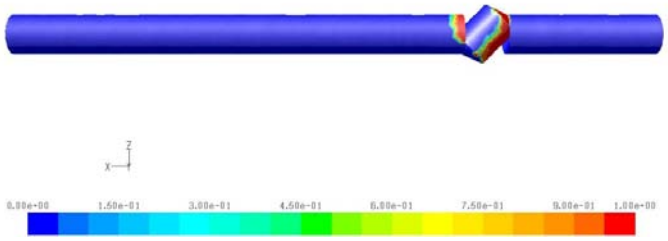

Fig. 37 Volume fraction of vapor phase 50 percent opening

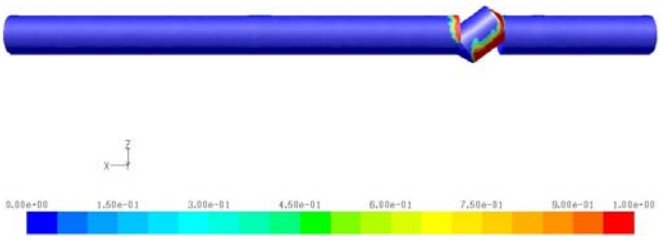

Fig. 38 Volume fraction of vapor phase for 60 percent opening

2. Results for 7.6 bar (110 psi) pressure drop:

a) *Graphs of pressure variation:*

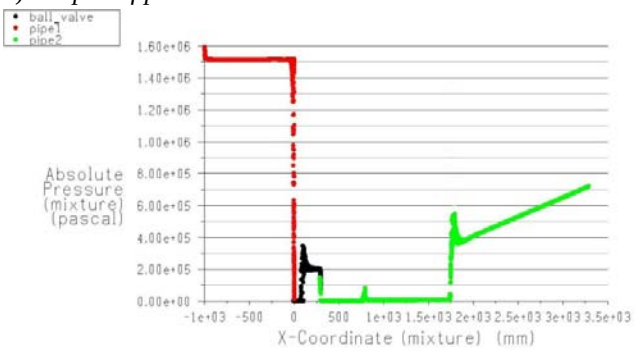

Fig. 39 Graph of absolute pressure variation for 10 percent opening

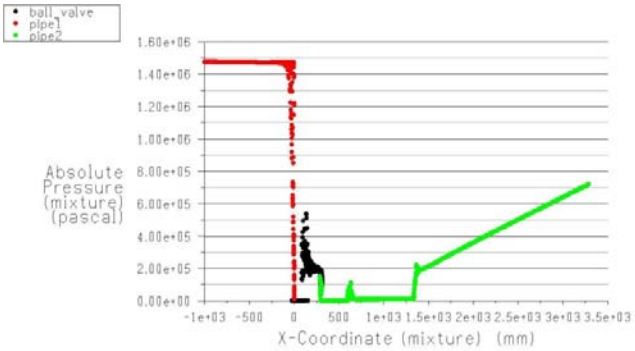

Fig. 40 Graph of absolute pressure variation for 20 percent opening

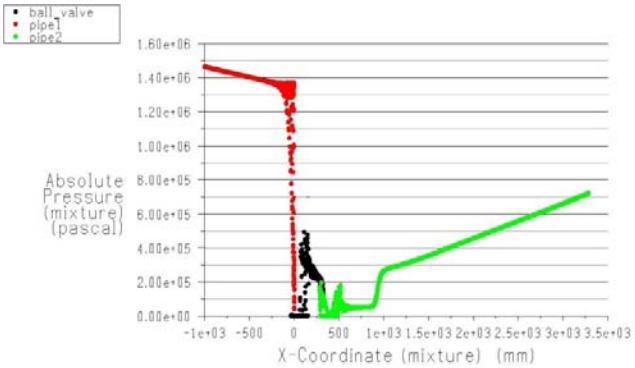

Fig. 41 Graph of absolute pressure variation for 30 percent opening

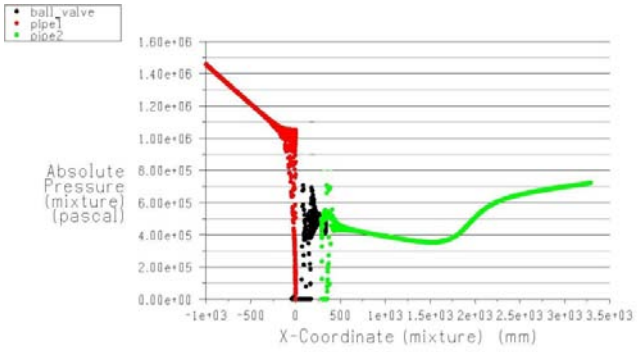

Fig. 42 Graph of absolute pressure variation for 40 percent opening

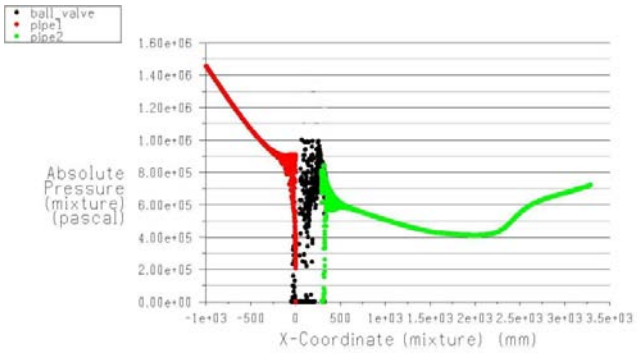

Fig. 43 Graph of absolute pressure variation for 50 percent opening

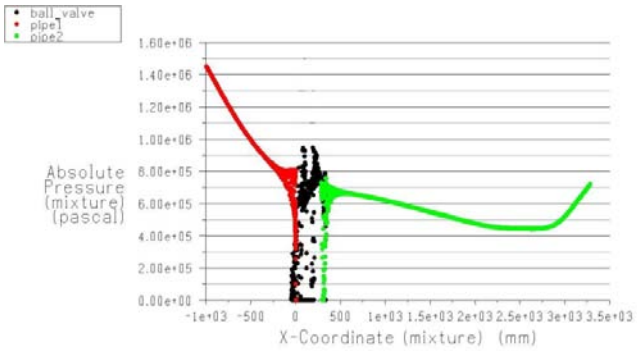

Fig. 44 Graph of absolute pressure variation for 60 percent opening

b) Velocity Contours on x-z plane:

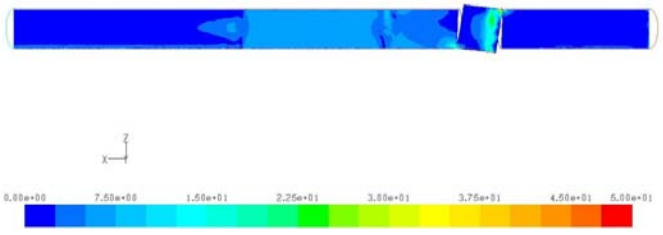

Fig. 45 Mixture velocity contour plot for 10 percent opening

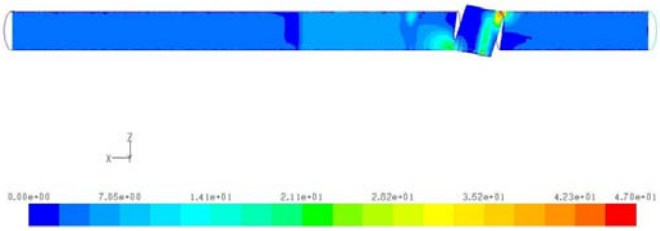

Fig. 46 Mixture velocity contour plot for 20 percent opening

Fig. 47 Mixture velocity contour plot for 30 percent opening

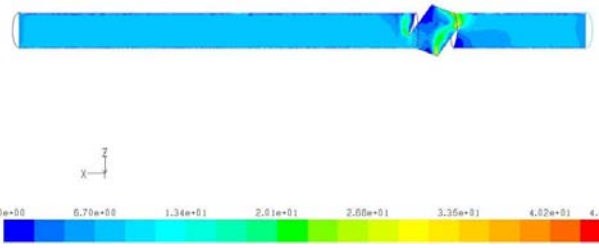

Fig. 48 Mixture velocity contour plot for 40 percent opening

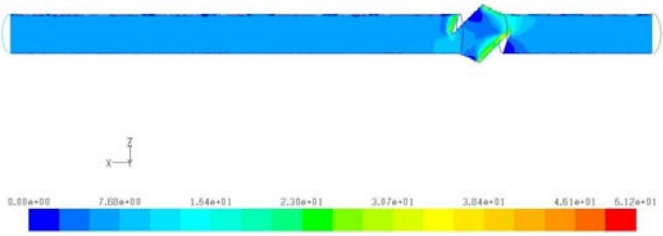

Fig. 49 Mixture velocity contour plot for 50 percent opening

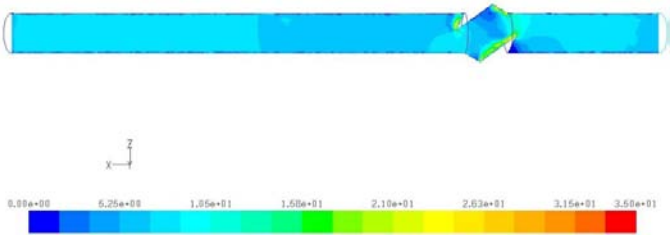

Fig.50 Mixture velocity contour plot for 60 percent opening

c) *Contour of Volume Fraction for Vapor Phase:*

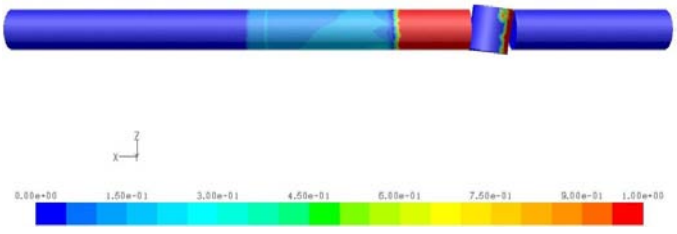

Fig. 51 Volume fraction of vapor phase for 10 percent opening

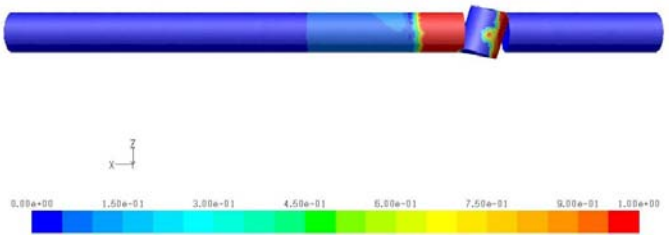

Fig. 52 Volume fraction of vapor phase for 20 percent opening

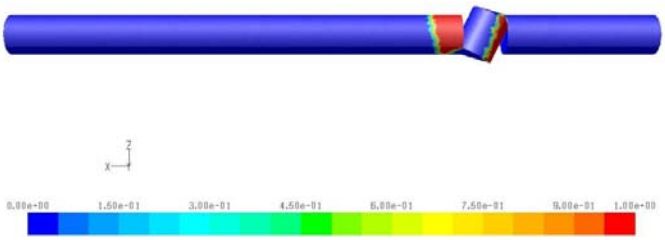

Fig. 53 Volume fraction of vapor phase for 30 percent opening

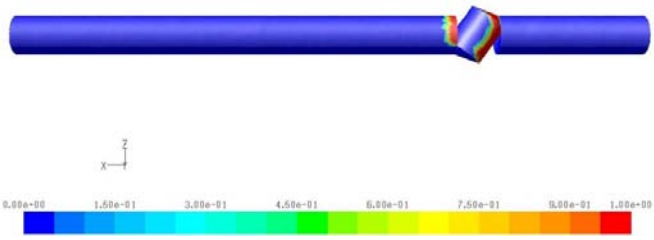

Fig. 54 Volume fraction of vapor phase for 40 percent opening

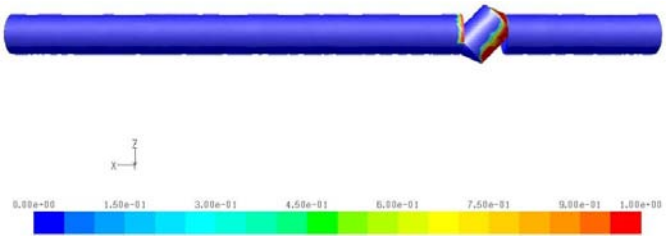

Fig. 55 Volume fraction of vapor phase for 50 percent opening

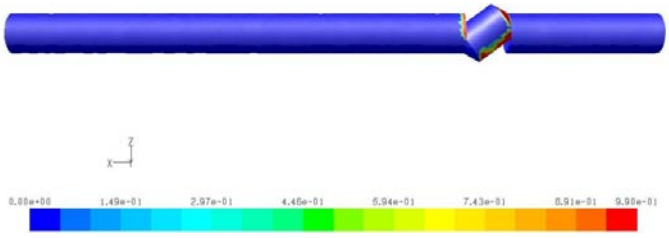

Fig. 56 Volume fraction of vapor phase for 60 percent opening

3. *Results of Cavitation Index:* Cavitation Index represents the intensity of cavitation process. Following figures shows graphs for cavitation index for the downstream side of the piping system, plotted for different pressure drops and at different percentage opening.

3.1. Cavitation Index for Constant Percentage Opening and Varying Pressure Drop, for Downstream Side:

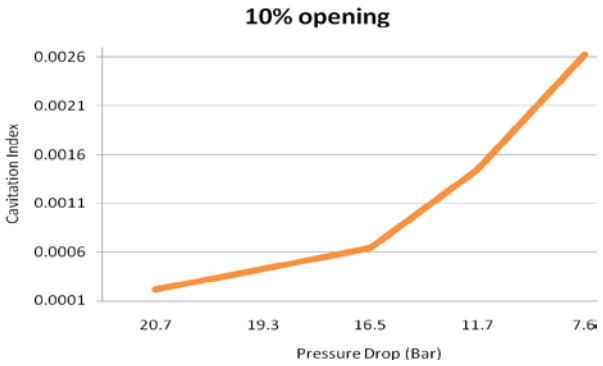

Fig. 57 Cavitation index for 10 percent opening and varying pressure drop

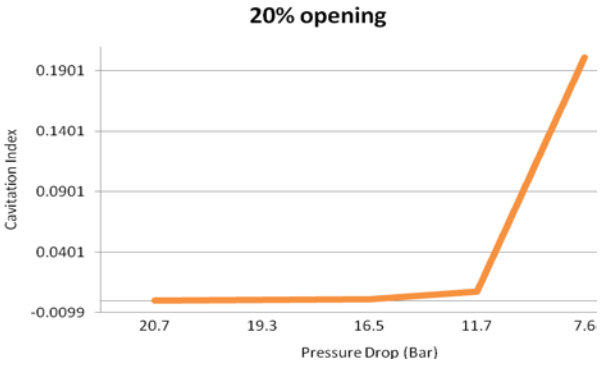

Fig. 58 Cavitation index for 20 percent opening and varying pressure drop

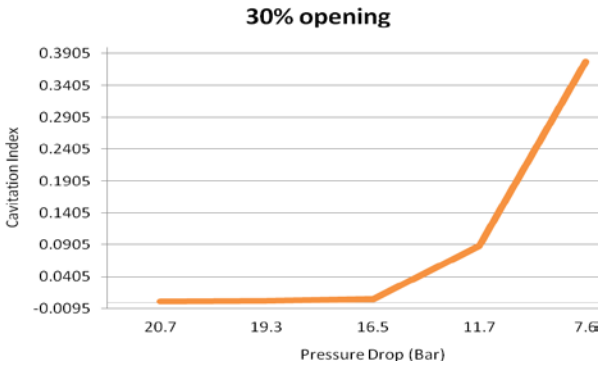

Fig. 59 Cavitation index for 30 percent opening and varying pressure drop

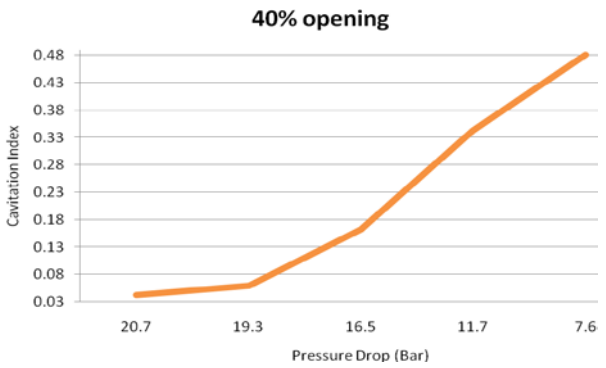

Fig. 60 Cavitation index for 40 percent opening and varying pressure drop

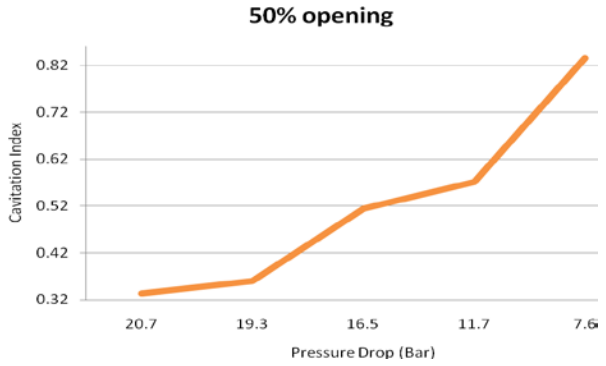

Fig. 61 Cavitation index for 50 percent opening and varying pressure drop

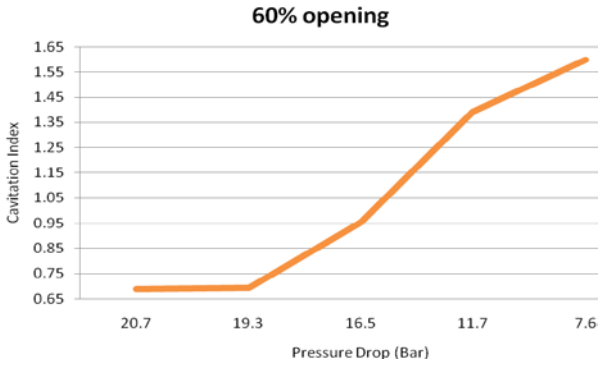

Fig. 62 Cavitation index for 60 percent opening and varying pressure drop

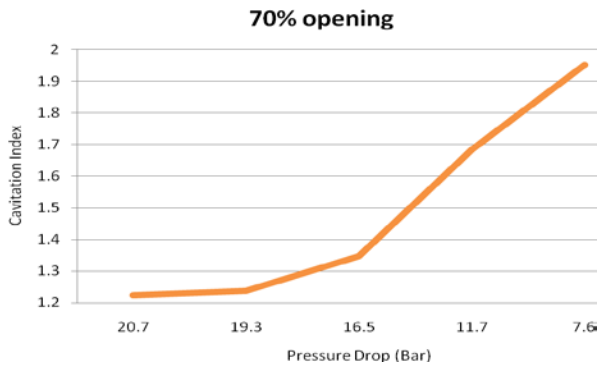

Fig. 63 Cavitation index for 70 percent opening and varying pressure drop

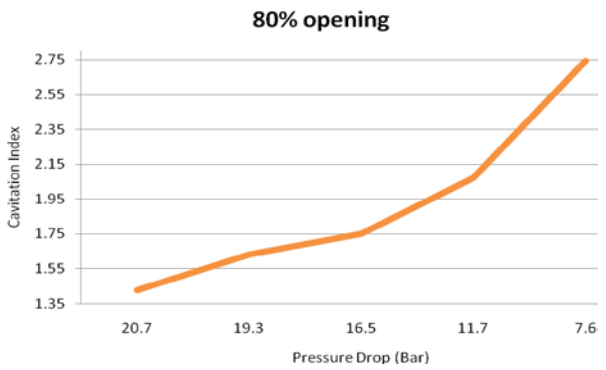

Fig. 64 Cavitation index for 80 percent opening and varying pressure drop

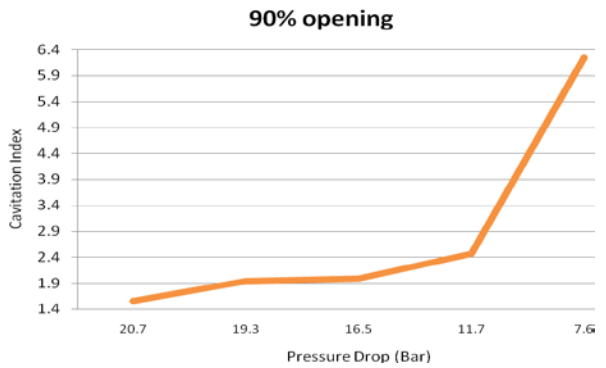

Fig. 65 Cavitation index for 90 percent opening and varying pressure drop

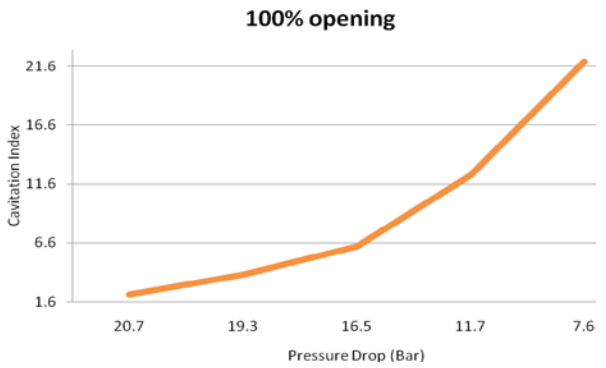

Fig. 66 Cavitation index for 100 percent opening and varying pressure drop

These curves indicate that for a particular fixed percentage opening as the pressure drop reduces, cavitation index increases. This indicates that cavitation index depends on pressure drop. Hence, cavitation reduces as pressure drop reduces.

3.2. Cavitation Index for Constant Pressure drop and Varying Percentage opening, for Downstream Side:

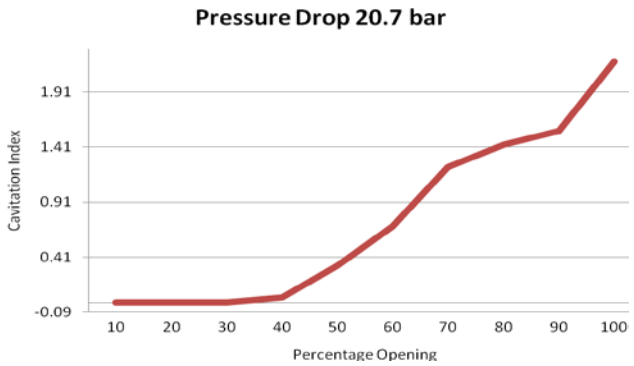

Fig. 67 Cavitation index for 20.7 pressure drop and varying percentage opening

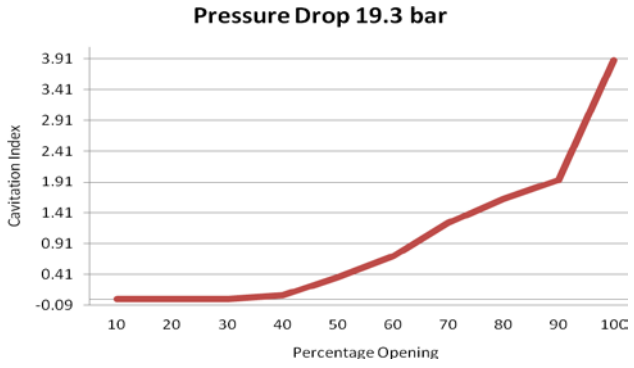

Fig. 68 Cavitation index for 19.3 pressure drop and varying percentage opening

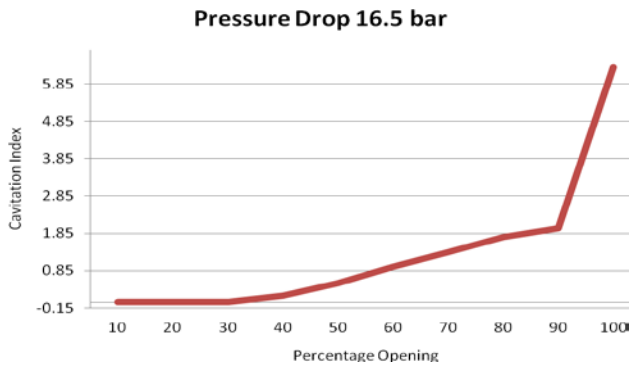

Fig. 69 Cavitation index for 16.5 pressure drop and varying percentage opening

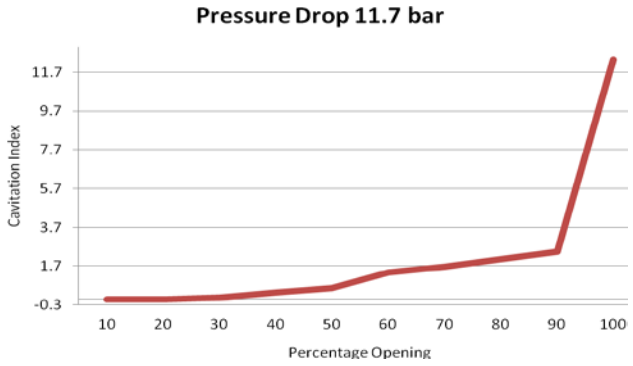

Fig. 70 Cavitation index for 11.7 pressure drop and varying percentage opening

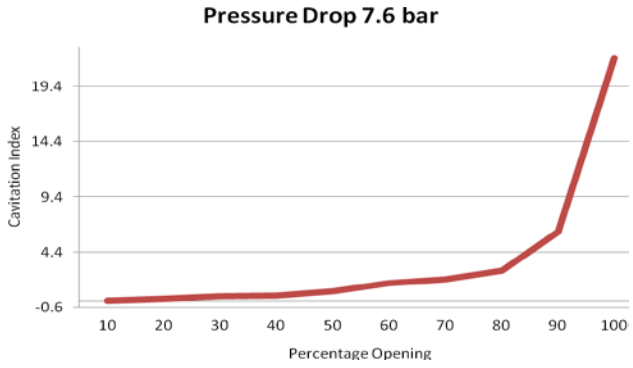

Fig. 71 Cavitation index for 7.6 pressure drop and varying percentage opening

Curves indicates that for a particular fixed pressure drop as percent opening reduces, cavitation index increases. This shows dependence of cavitation index on percentage opening. Cavitation increases as valve is closed.

V. Conclusion

- As valve is closed its sizing coefficient reduces.
- Torque coefficient raises to a maximum point and then reduces, in this study it is maximum at 80 percent opening.
- Hydrodynamic torque increases to a peak point and falls as valve is closed. It is maximum at 60% opening.

- Though maximum torque coefficient is obtained at 80 percent of valve opening, it does not mean that hydrodynamic torque is maximum at the same percentage opening.
- Cavitation Index depends both on pressure drop and percentage opening.
- A high intensity cavitating turbulent flow was observed at 20.7 bar (300 psi) and 10 percent valve opening. In order to protect this valve from cavitation when such conditions prevails, proper measure must be used, for example, Anti Cavitation Trims, these causes the pressure to drop in stages and do not allow pressure to fall below the vapor pressure.
- Hence while designing the valve systems designer must consider the entire range of sizing coefficient, hydrodynamic torque and torque coefficient and cavitation index.

ACKNOWLEDGMENT

Yogesh Gawas thanks, Dr. Vilas R. Kalamkar, Mr. Vijay Mali, and Centre for Computational Technologies (CCTech) Pvt. Ltd., Pune, India, for their assistance for the successful completion of this study by providing the necessary resources.

REFERENCES

[1] M. J. Chern and C. C. Wang, "Control of volumetric flow-Rate of ball valve using V-port," *Journal of Fluid Engineering.*, vol. 126, pp. 471–481, May. 2004.

[2] P. Merati, M. J. Macelt, and R. B. Erickson, "Flow investigation around a V-sector Ball Valve," *Journal of Fluid Engineering.*, vol. 118, pp. 662-671, 2001.

[3] C. Huang, and R. H. Kim, "Three-dimensional analysis of partially open butterfly valve flows," *Journal of Fluid Engineering.*, vol. 123, pp. 562-568, 1996.

[4] C. van Lookeren Campagne, R. Nicodemus, G. J. de Bruin, and D. Lohse, "A method for pressure calculation in Ball valve containing bubbles," *Journal of Fluid Engineering.*, vol. 124, pp. 765-771, 2002.

[5] X. Song, and Y. C. Park, "Numerical analysis of butterfly valve-prediction of flow coefficient and hydrodynamic torque coefficient," *World Congress on Engineering and Computer Science.*, October. 2007.

[6] S. Bernad, R. Susan-Resiga, S. Muntean, I. Anton, "Numerical analysis of the cavitating flows," *Proceedings of the Romanian Academy, Series A,.*, vol. 7, November. 2006.

[7] "Flowserve cavitation control," *Flowserve Corporation, USA.*, FCD-FCENBR0068-01.

[8] ANSYS FLUENT 12.0 User's Manual, ANSYS, Inc.

[9] J. P. Tullis, "*Hydraulics of Pipelines: Pumps, Valves, Cavitation, Transient,*" 1st ed., John Wiley & Sons, Inc, 1989, pp. 81–168.

[10] P. L. Skousen, "Valve Handbook," McGraw-Hill, 1997, pp.221-478.